TISSUE ENGINEERING: Part A Volume 29, Numbers 21 and 22, 2023 © Mary Ann Liebert, Inc. DOI: 10.1089/ten.tea.2023.0104



Open camera or QR reader and scan code to access this article and other resources online.



Deciphering the Cell-Specific Effect of Osteoblast-Macrophage Crosstalk in Periodontitis

Diego Jacho, Parto Babaniamansour, Raquel Osorio, PhD, Adano, PhD,

In periodontitis, the bone remodeling process is disrupted by the prevalent involvement of bacteria-induced proinflammatory macrophage cells and their interaction with osteoblast cells residing within the infected bone tissue. The complex interaction between the cells needs to be deciphered to understand the dominant player in tipping the balance from osteogenesis to osteoclastogenesis. Yet, only a few studies have examined the crosstalk interaction between osteoblasts and macrophages using biomimetic three-dimensional (3D) tissue-like matrices. In this study, we created a cell-laden 3D tissue analog to study indirect crosstalk between these two cell types and their direct synergistic effect when cultured on a 3D scaffold. The cell-specific role of osteoclast differentiation was investigated through osteoblast- and proinflammatory macrophage-specific feedback studies. The results suggested that when macrophages were exposed to osteoblasts-derived conditioned media from the mineralized matrix, the M1 macrophages tended to maintain their proinflammatory phenotype.

Further, when osteoblasts were exposed to secretions from proinflammatory macrophages, they demonstrated elevated receptor activator of nuclear factor- κB ligand (RANKL) expression and decreased alkaline phosphate (ALP) activities compared to osteoblasts exposed to only osteogenic media. In addition, the upregulation of tumor necrosis factor-alpha (TNF- α) and c-Fos in proinflammatory macrophages within the 3D matrix indirectly increased the RANKL expression and reduced the ALP activity of osteoblasts, promoting osteoclastogenesis. The contact coculturing with osteoblast and proinflammatory macrophages within the 3D matrix demonstrated that the proinflammatory markers (TNF- α and interleukin-1 β) expressions were upregulated. In contrast, anti-inflammatory markers (c-c motif chemokine ligand 18 [CCL18]) were downregulated, and osteoclastogenic markers (TNF receptor associated factor 6 [TRAF6] and acid phosphatase 5, tartrate resistant [ACP5]) were unchanged. The data suggested that the osteoblasts curbed the osteoclastogenic differentiation of macrophages while macrophages still preserved their proinflammatory lineages. The osteoblast within the 3D coculture demonstrated increased ALP activity and did not express RANKL significantly different than the osteoblast cultured within a 3D collagen matrix without macrophages. Contact coculturing has an anabolic effect on bone tissue in a bacteria-derived inflammatory environment.

Keywords: periodontitis, osteoclastogenesis, osteoblasts, osteoclasts, macrophages, receptor activator of nuclear factor-κB ligand (RANKL), conditioned-media culturing, direct coculturing

¹Department of Bioengineering, University of Toledo, Toledo, Ohio, USA.

²Department of Dentistry, University of Granada, Colegio Máximo de Cartuja, Granada, Spain.

³Instituto de Investigación Biosanitaria ibs, University of Granada, Granada, Spain.

⁴Department of Biological Sciences, University of Toledo, Toledo, Ohio, USA.

Impact Statement

This study investigated the interaction between osteoblasts and proinflammatory macrophages in periodontitis using a three-dimensional (3D) tissue analog. The results showed that exposure of macrophages to osteoblasts-derived conditioned media maintained their proinflammatory phenotype. In contrast, exposure of osteoblasts to macrophage secretions decreased alkaline phosphate (ALP) activity and increased receptor activator of nuclear factor-kB ligand expression, promoting osteoclastogenesis. Coculturing of osteoblasts and macrophages within the 3D matrix increased ALP activity and had an anabolic effect on bone tissue. These findings suggest that osteoblasts can curb the osteoclastogenic differentiation of macrophages, while macrophages preserve their proinflammatory lineages in a bacteria-derived inflammatory environment.

Introduction

NE OF THE MOST PREVALENT chronic inflammatory diseases in modern dentistry is periodontitis, associated with destroying the tooth-supporting tissues, eventually leading to tooth loss. Macrophages, as innate immune cells, play a key role in the development and progression of periodontitis. In the early stages of periodontitis, blood circulating monocytes are activated by bacteria in dental plaque, rushed to the infected area, and turned into the naïve macrophages (M0).²⁻⁴ Upon extravasating into infected tissue, M0 macrophages differentiate into proinflammatory phenotype (M1) and release proinflammatory signaling molecules, such as tumor necrosis factor-alpha (TNF-α) and interleukin-1 (IL-1), to remove the bacteria. 5-7 However, if the infection is not resolved, the continued presence of bacteria-induced M1 activation can lead to the destruction of the supporting structures of the teeth, including the gums, periodontal ligament, and alveolar bone through starting osteoclastogenesis and disruptive bone remodeling process.

Osteoblasts are responsible for bone formation and remodeling within the alveolar bone. They are also activated by proinflammatory macrophages and the release of proinflammatory signaling molecules and prominent osteoclast markers. M1-induced activation leads to the synthesis and secretion of enzymes from osteoblast, such as matrix metalloproteinases (MMPs), that can break down the extracellular matrix of bone and lead to the resorption of bone tissue. The *in vitro*, *in vivo*, and clinical studies further demonstrated that the presence of M1 macrophages triggers osteoblasts to express the receptor activator of nuclear factor-κB ligand (RANKL), a soluble cytokine essential for osteoclast differentiation from M1 macrophages.

Mounting evidence suggests that the proinflammatory macrophages and osteoblasts or mesenchymal stem cells interact and influence each other's function ^{19–32} toward osteogenesis. A bidirectional deep and complex crosstalk between the proinflammatory macrophages and osteoblasts mediates bone loss. It significantly contributes to the progression of periodontitis and many inflammatory osteolytic diseases. ¹⁷ Yet, it remains relatively unexplored and challenging to decipher the solo effect of each cell type on other's differentiation and functions using biomimetic culturing models.

In this respect, most *in vitro*, macrophage/osteoblast coculture models use two-dimensional (2D) indirect coculturing using a transwells system or direct coculturing using contact culturing in a culture dish.^{33–35} These coculture models are convenient since they provide a controlled environment to study cell–to–cell interaction and the influence of these cells on each other's function. However, current macrophage/osteoblast coculturing models have been unable to identify the cell-specific effect on bone remodeling and detrimental osteoclastogenesis. Specifically, it is unknown whether osteoclastogenesis results from inflammatory cytokine secreted by M1 macrophages and the stimulatory effect of osteoblast-induced osteoclastogenic markers, understanding the dominant cell type in macrophage/osteoblast crosstalk toward osteoclastogenesis.

To address these issues, a well-defined 3D *in vitro* conditioned media platform and contact coculturing within a 3D matrix can be beneficial to investigate the role of individual cell type and their synergistic effect in osteolytic bone diseases, including periodontitis. To this end, this study is aimed to understand the respective roles of M1 macrophages and osteoblast in macrophage differentiation and osteoblast function toward osteoclastogenesis. We utilized a biomimetic-conditioned media model and 3D contact culturing to study which cell type was responsible for phenotypic changes in proinflammatory macrophages toward osteoclast.

Materials and Methods

Cell culturing and 3D cell-laden collagen scaffold synthesis

Before preparing 3D cell-laden collagen scaffolds, the human fetal osteoblast cells (hFOB; ATCC, USA), hFOBgreen fluorescence protein (GFP) tagged, and human bloodderived U937 monocytes (U937; ATCC) were populated separately. The hFOB osteoblast cells were populated in Ham's F12 medium Dulbecco's modified Eagle's medium (DMEM; ATCC) supplemented with 10% fetal bovine serum (FBS), 0.3 mg/mL G418, and 50 µg/mL ascorbic acid at 34°C and 5% CO₂ for 2 weeks. The U937 monocytes (U937; ATCC) were populated in Roswell Park Memorial Institute (RPMI) media supplemented with 10% FBS and 1% penicillin-streptomycin at 37°C and 5% CO₂ before being differentiated into naïve macrophages via incubation with 100 ng/mL PMA for 24h. After phorbol 12-myristate 13acetate (PMA) treatment, naïve macrophages were differentiated into M1 (proinflammatory) via incubation with 100 ng/mL lipopolysaccharide (LPS) and 20 ng/mL interferongamma for 24 h.

The 3D scaffolds were synthesized using collagen type-I. The neutralized collagen solution was prepared from $8.9 \, \text{mg/mL}$ collagen type-I solution (Corning, USA) with a pH of ~ 3.4 through mixing with 1 M sodium hydroxide, phosphate buffer solution (PBS), and cell in media suspension to a final collagen concentration of $3 \, \text{mg/mL}$, using our well-established protocols. $^{1-6}$ Then, human osteoblast or M1 macrophages were plated in a petri dish or encapsulated

within the 3D collagen scaffolds at a 10^6 cells/mL cell density depending on the experimental set-ups and incubated at 37°C and 5% CO₂. The size of the 3D collagen scaffolds was 0.5 mL across all groups, and the scaffolds were incubated in 6-well plates. Additionally, the same number of cells as in scaffolds were seeded per petri dish for all the 2D cultures (Fig. 1).

Conditioned media (indirect) and direct coculturing platform

Following the synthesis and incubation of 3D scaffolds, indirect coculture between both cell lines was completed via media transfer. The 0.5 mL 3D scaffolds were synthesized with either hFOB or M1 macrophages at a 10^6 cells/mL cell density in a six-well plate ($n\!=\!3$). Each 3D collagen scaffold was cultivated with DMEM or RPMI for osteoblast or M1 macrophages, respectively. On day 4, three 3D hFOB scaffolds were characterized for scanning electron microscopy (SEM), alkaline phosphate (ALP) activity, and histology staining.

Then, the media from either 3D hFOB or 3D M1 scaffolds was collected daily for 7 days, mixed with complete fresh media (1:1), and transferred to the opposite cell line growing on a petri dish. In addition, complete fresh media was replaced on the scaffolds every 3 days to allow cells to be refurbished with nutrients. For the direct coculture, hFOB-GFP and M1 cells were encapsulated in 0.5 mL scaffolds at a 1:1 ratio (10⁶ cells/mL cell density) and incubated for 7 days at 37°C and 5% CO₂. During direct coculture, the media used for cultivation was a 1:1 mixture of complete DMEM and RPMI medium. The medium was replaced every 3 days.

Alkaline phosphate activity

The ALP activity of the 2D samples and 3D scaffolds was evaluated using a fluorometric ALP assay kit (Abcam, USA). ALP cleaves the phosphate group of the nonfluorescent 4-methylymbelliferyl phosphate disodium salt (MUP) substrate resulting in an intense fluorescent signal. Before ALP analysis, the samples were washed, encapsulated cells within the scaffolds were liberated by snap freezing the scaffolds, cells were counted, and a concentration of 0.5 M cells per solution was homogenized on the ALP assay buffer. The samples were centrifuged, and the supernatant was collected for assay. The MUP (5 mM) substrate and assay buffer were added to the supernatant in a 96-well plate, and the solutions were incubated for 30 min at 25°C, protected from light. A stop solution was used, and the 4-methylumbelliferone (4-MU) production was determined by measuring $E_x/E_m = 360/440 \text{ nm}$ using a microplate reader (SOFTmax Pro). A standard curve was established using a serial dilution of the ALP enzyme to convert the measured absorbance to a MU value. Results were normalized to the ALP 4-MU standard curve following the manufacturer's protocol and the ALP 4-MU standard curve.

Matrix organization and mineral mapping

The morphological and mineral content changes due to *in situ* mineralization were examined using SEM (Hitachi, USA). Briefly, on characterization day, the 3D scaffolds were cut and fixed with 4% paraformaldehyde in PBS for 30 min. After fixation, the samples were dehydrated first in sequential ethanol

solutions with increasing concentrations from 30% to 100% for 15 min each. Dehydration was then continued by submerging samples into sequential ethanol/hexamethyldisilane solutions from 30% to 100% for 10 min each for image quality enhancement. The samples were then air-dried overnight. The dried samples were then gold sputter coated for visualization and mineral content measurement through energy dispersive X-ray spectroscopy (EDS).

Histological analysis

The cellular content and encapsulated cells within the 3D scaffolds were visualized using histological analysis. On characterization day (day 7), the scaffolds were removed and washed with PBS for 10 min. Then, samples were incubated in 10% formalin overnight, dehydrated using an ethanol gradient, and cleared with xylene before embedding in paraffin. The paraffin-embedded samples were sectioned at 5 μ m thickness using a microtome and mounted on microscope slides. Hematoxylin and eosin (H&E) and Masson's trichrome were used to visualize the cells and collagen fibers, respectively.

Gene expression analysis

To analyze the specific phenotypic changes in osteoblasts and M1 macrophages during indirect and direct culture, we analyzed gene expression using quantitative real-time polymerase chain reaction (RT-qPCR). In brief, on the characterization day, the 2D samples or 3D scaffolds were mechanically disrupted, and RNA extraction was performed using TRIzol reagent (ThermoFisher, USA). For direct co-culture, the 3D scaffolds were disturbed, and cells were released using collagenase type IV (ThermoFisher). Subsequently, the resulting solution was prepared for fluorescence-activated cell sorting (FACS). Cell populations were gated on the BD FACSAria[™] Fusion Sorter based on viability and a positive signal for ATTO-488. Each cell line was directly collected in TRIzol reagent.

The isolated RNA was then reverse-transcribed into complementary DNA using the Superscript IV kit (Invitrogen, USA) following the manufacturer's protocols. RT-PCR was carried out using TaqMan SYBR (Bio-Rad, USA) in the iCycler iQ detection system (Bio-Rad). The relative gene expression, indicating the fold difference between treated and control samples, was determined using the $\Delta\Delta Ct$ method. Glyceraldehyde-3-phosphate dehydrogenase was the housekeeping gene to normalize the data. The primer sequences for each gene were designed using the NCBI primer blast software and synthesized by Integrated DNA Technologies (USA). The complete list of genes and their corresponding primer sequences can be found in Table 1.

Immunofluorescence and immunohistochemistry

Immunofluorescence and immunohistochemistry staining assays were performed on both the control and conditioned media (Macrophages) and the 3D scaffold samples to verify the gene expression data at the protein level. On characterization day, the slides were extracted from the wells, fixed in 4% paraformaldehyde, quenched with an ammonium chloride solution, and then permeabilized with Triton X-100. Samples were washed and blocked in 2.5% goat serum and

	_		_		~ -	
TARIE 1	FORWARD AND	REVERSE PRIMI	EDS EOD REAL.	TIME POLVM	TEDASE C'HAIN R	FACTION

Gene	Forward primer	Reverse primer	References
RANKL	TCCATGTTCGTGGCCCTCCT	TGCAGTGAGTGCCATCTTCTG	18
ACP5	CGACGCAGGGACTGAAGG	TCCATCCAGGGGGAGACACA	4
TRAF6	AGAGTTTGCCGTCCAAGCAG	GCACACAAAGAAAGCTGGGTCC	19
NF - κB	GGGGCTGTGCCGGTTGAAA	AGATGTCCTCCTGCGTCTCG	19
ALPL	CTATCCTGGCTCCGTGCTCC	GCCACGTTGGTGTTGAGCTT	4
IL-1β	AGCCATGGCAGAAGTACCTG	CCTGGAAGGAGCACTTCATCT	20
TNF-α	AGAGGGAAGAGTTCCCCAGGGAC	TGAGTCGGTCACCCTTCTCCAG	4, 20
CD163	TCTGTTGGCCATTTTCGTCG	TGGTGGACTAAGTTCTCTCCTCTTGA	20
CCL18	AAGAGCTCTGCTGCCTCGTCTA	CCCTCAGGCATTCAGCTTAC	20
MMP3	CAGCCAACTGTGATCCTGCT	CTTCATATGCGGCATCCACG	20
GAPDH	AGAAGGCTGGGGCTCATTTG	AGGGCCATCCACAGTCTTC	20
c-FOS	CTTTGCAGACCGAGATTGCC	ATCAGGGATCTTGCAGGCAG	53

ACP5, acid phosphatase 5, tartrate resistant; ALPL, alkaline phosphatase, biomineralization associated; CCL18, c-c motif chemokine ligand 18 fos proto-oncogene; GAPDH, glyceraldehyde 3-phophate dehydrogenase; $IL-1\beta$, interleukin-1β; MMP3, matrix metalloproteinase 3; $NF-\kappa B$, nuclear factor kappa B; RANKL, receptor activator of nuclear factor- κB ligand; $TNF-\alpha$, tumor necrosis factor-alpha; TRAF6, TNF receptor associated factor 6.

0.2% Tween in PBS for 10 min, followed by 20 min blocking in 0.4% bovine serum albumin (BSA) and 0.2% Tween in PBS.

After blocking, slides were incubated overnight at 4°C in mouse anti-CD80 (1:100) (Invitrogen; TA501575). The next day, slides were washed thrice with PBS and 0.2% Tween solution for 30 min and blocked in 0.4% BSA and 0.2% Tween solution for 20 min at room temperature (RT). After blocking, samples were incubated for 2-3 h at RT with Alexa Flour 594-goat anti-mouse IgG (1:100) (A32730; ThermoFisher), Alexa Flour 647-goat anti-rabbit IgG (1:100) (A31634, Thermofisher), and Alexa Flour 488 Phalloidin (1:50) (ThermoFisher: A12379). 4'.6-Diamidino-2-phenylindole (DAPI) dye (1:1000) was used to stain for nuclei. Slides were washed with 0.2% Tween and mounted in Permount mounting media (Permount, USA). The samples were left in the dark overnight at 4°C before imaging. Using a microtome, a similar staining protocol was used for 3D-scaffold samples after sectioning at 40 µm thickness.

Samples were imaged using a 63×oil or 20×airy objective with a Leica Stellaris 5 confocal system equipped with HyD detectors and the LASX software. The confocal images obtained were then processed and analyzed using ImageJ and CellProfiler. Briefly, confocal images from at least three independent studies were processed to measure each cell's filamentous actin (F-actin) and CD80 intensity. The segmentation of cells was achieved on CellProfiler using both signals (Hoescht and F-actin), and the pipeline obtained was used to measure the F-actin and CD80 intensity. The relative mean intensity was obtained from Cell-Profiler and imaged using a bell-shaped image in RStudio.

Statistical analysis

Statistical analysis was conducted using RStudio. Statistical significance was analyzed using one-way analysis of variance and *post-hoc* analysis (Tukey test) or Student's *t*-test where appropriate. Data were analyzed for normalization using RStudio, and proper statistical analysis was selected. The data are reported as the mean \pm SE. Symbols on top of each bar profile summarize Tukey's *post hoc* analysis of at least three independent studies (p < 0.05). IRB protocol #500086.

Results

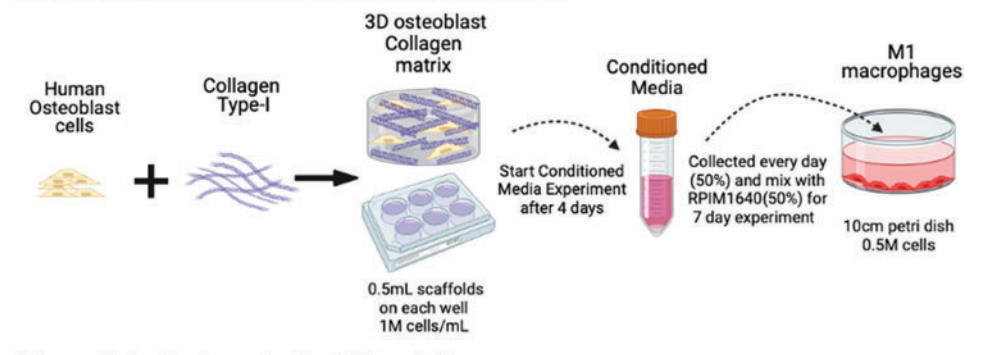
Osteoblast-specific feedback on macrophage differentiation

To understand the osteoblast-specific effect on macrophage differentiation, the macrophages were cultured with conditioned media from the osteoblast-laden 3D mineralized matrix (3D hFOB) for 7 days (Fig. 1). Before collecting conditioned media from 3D hFOB culturing, it was crucial to prove that human osteoblasts (hFOBs) residing within the 3D matrix were healthy and depositing calcium into the matrix. Overall, the data in Figure 2 validated the mineralized matrix formation within the osteoblast-laden 3D matrix. Figure 2A shows the representative SEM image of the 3D hFOB. The EDS analysis was conducted on SEM images to identify the mineral contents within the 3D hFOB matrix. The EDS spectral graph (Fig. 2B) demonstrates a pronounced peak at 3.50–3.70 keV corresponding calcium, indicating dominant calcium presence within the 3D hFOB matrix. The calcium mineral mapping (Fig. 2C) also demonstrated the calcium mineral deposition within the 3D hFOB matrix by encapsulated osteoblast cells. The spectral analysis data were further confirmed with ALP activity assessment and von Kossa staining of the 3D hFOB matrix (Fig. 2D-F).

The ALP data demonstrated that on the same characterization day, hFOB within a 3D matrix had a statistically significant (p<0.05) ALP activity compared to hFOB cultured within a 2D surface using the same osteogenic media (Fig. 2D). The histological images further demonstrated the calcium mineral deposits as brown/dark spots, while the hFOB nuclei were counterstained with red and their cytoplasm in pink (Fig. 2E, F). The yellow arrows (Fig. 2F) indicate the representative cells and calcium deposits in the von Kossa-stained slides. In addition, Figure 2G–K presents the SEM, EDS, and calcium mapping results of acellular scaffolds treated with conditioned media. The Ca mapping clearly illustrates that the media contains calcium; however, the observed amounts are significantly lower than the 3D hFOB matrix, which contains cells.

It is well established that osteoblast-derived cytokines, including nuclear factor kappa B (NF-κB) and RANKL,

Osteoblast-specific feedback on macrophages differentiation



M1-specific feedback on osteoblast differentiation

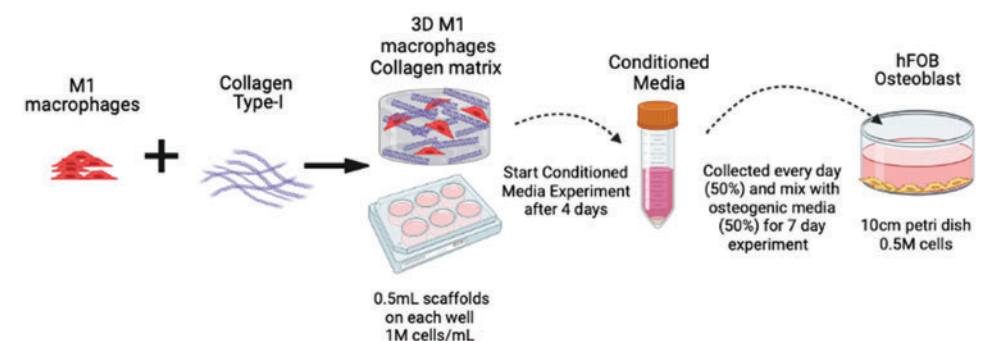
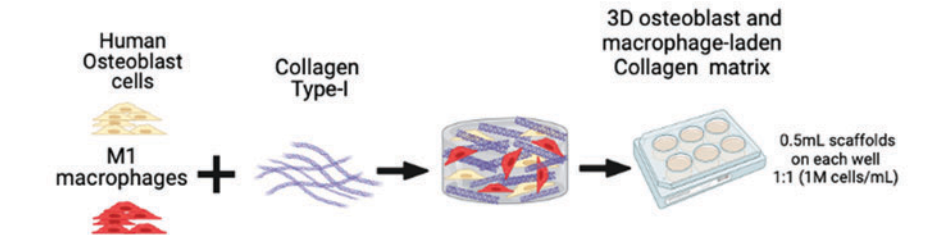


FIG. 1. The schematic representations of cell-specific and coculture study experimental set-ups. M1, proinflammatory macrophages. Color images are available online.

Co-Culture Effect on Macrophage and Osteoblast differentiation



modulate the macrophage differentiation toward osteoclast precursor cells and initiate osteoclastogenesis. 36,37 Thus, the RANKL and NF-κB mRNA expressions from the osteoblasts within the mineralized 3D hFOB matrix were assessed upon confirming the mineralized matrix formation. Figure 3 demonstrates that while NF-κB expression was significantly upregulated for the osteoblast within the 3D hFOB matrix compared to counterparts cultured on a 2D surface, the RANKL expression was not changed.

Next, the effect of osteoblast-derived conditioned media on phenotypic changes in inflammatory macrophages was assessed. Figure 4 demonstrates the mRNA expression of pro- and anti-inflammatory markers, osteoclast markers, and immunohistochemistry (IHC) staining of macrophages cultured in regular complete media (M1) and macrophages cultured in osteoblast-derived conditioned media (M1 CM).

The gene expression analysis demonstrated that there were no statistical differences in proinflammatory (TNF- α and IL-1 β) and anti-inflammatory markers (c-c motif chemokine ligand 18 [CCL18]) expressions between macrophages cultured in regular complete media (M1) and macrophages cultured in osteoblast-derived conditioned media (M1 CM) (Fig. 4A). The gene expression result indicated that osteoblast-derived con-

ditioned media preserve the proinflammatory phenotype of M1 macrophages rather than differentiating them to the anti-inflammatory phenotype (M2). This was further confirmed with IHC staining (Fig. 4B) of CD80, a prototypical and widely accepted M1 marker. The immunofluorescence images (Fig. 4B) and relative fluorescence intensity analysis (Fig. 4C) demonstrated no statistically significant differences in surface expressions of CD80 and F-actin stress fibers between macrophages cultured in regular media (M1) and osteoblast-derived conditioned media (M1 CM). The osteoblast-derived conditioned media preserved the proinflammatory lineage of macrophages.

In this respect, the expression of osteoclastogenic markers following osteogenic-conditioned media culturing was further investigated to understand whether osteoblast-derived conditioned media promoted the osteoclastogenic differentiation of M1 macrophages.

Figure 5 demonstrates the gene expressions of osteoclastogenic markers of macrophages cultured in regular media (M1) and osteoblast-derived conditioned media (M1 CM). The prominent osteoclast markers MMP3 and TNF receptor associated factor 6 (TRAF6) were significantly (p<0.05) upregulated for M1 CM macrophages, while no

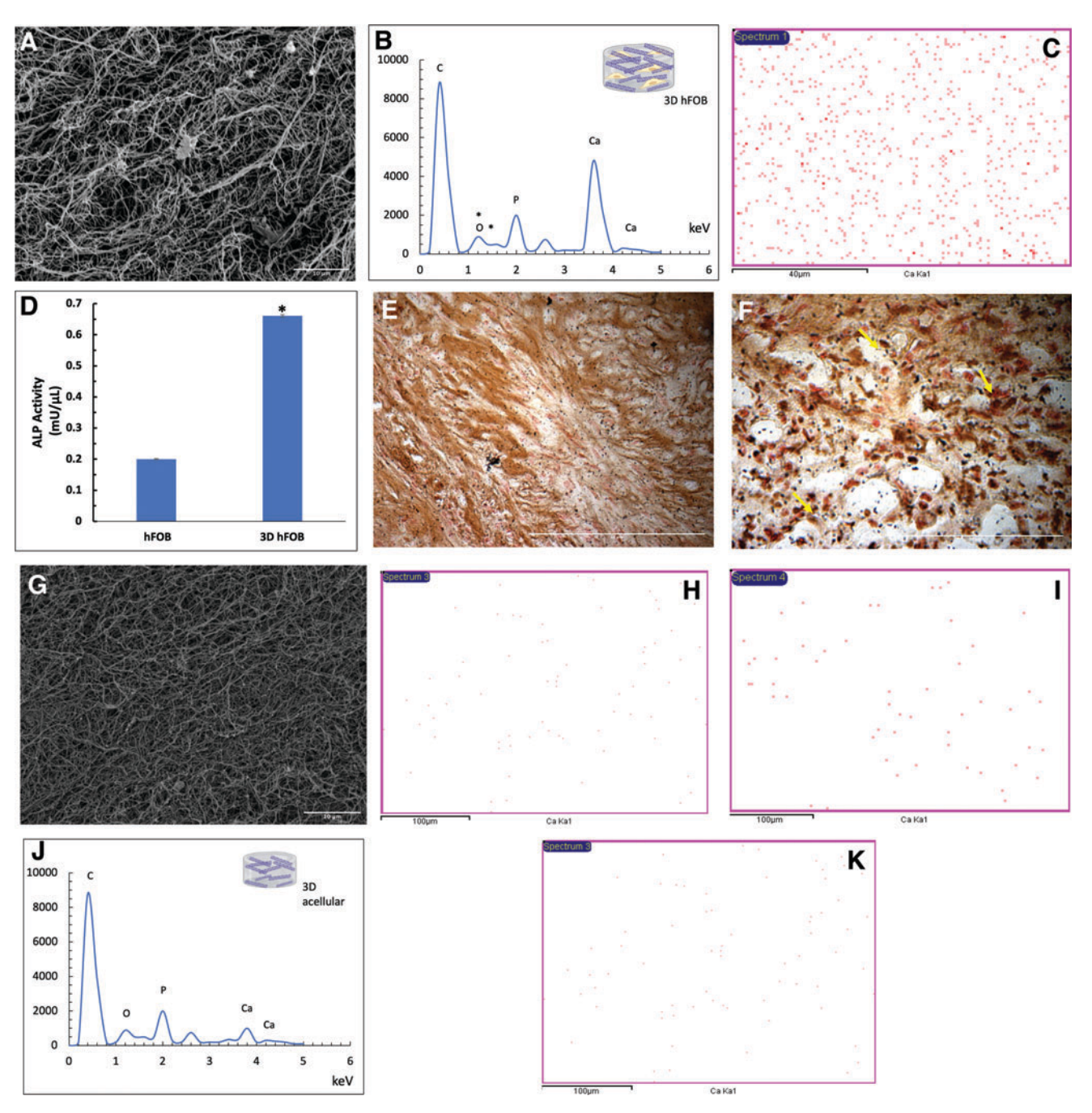


FIG. 2. Structural, spectral, and biological analyses of 3D hFOB mineralized matrix and acellular matrix. (**A**) SEM image of osteoblast within 3D matrix, scale bar=10 μ m. (**B**) EDS spectral analysis of 3D hFOB mineralized matrix. (**C**) Distribution maps of calcium minerals (*red dots*) within 3D hFOB matrix, scale bar=40 μ m. (**D**) ALP activity of hFOB within 3D matrix; the symbol "*" indicates significant difference with p < 0.05 (n = 3). (**E**) Von Kossa staining of 3D hFOB matrix histological slides, scale bar=20 μ m. (**F**) Magnified images of calcium deposition (*yellow arrows*) from von Kossa staining of 3D hFOB matrix histological slides, scale bar=20 μ m. (**G**) SEM image of acellular scaffold, scale bar=10 μ m. (**H**) Distribution maps of calcium minerals (*red dots*) of acellular scaffold treated with M1 media. (**I**) Distribution maps of calcium minerals (*red dots*) of acellular scaffold treated with 1:1 mix media, scale bar=100 μ m. ALP, alkaline phosphate; EDS, energy dispersive X-ray spectroscopy; hFOB, human fetal osteoblast cells; SEM, scanning electron microscopy. Color images are available online.

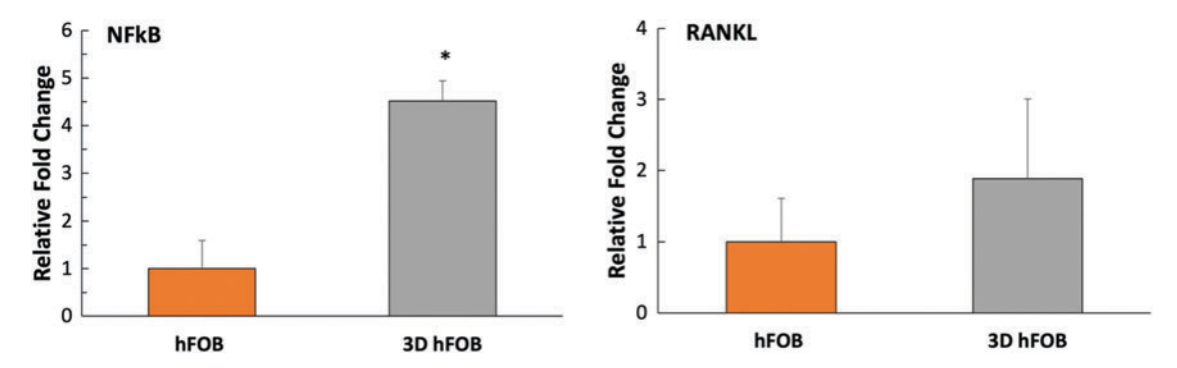


FIG. 3. Gene expression of osteoclast activity markers NF- κ B, and RANKL from osteoblast. The symbol "*" indicates significant difference with respect to osteoblast cells with osteogenic media with p < 0.05 (n = 3). NF- κ B, nuclear factor kappa B; RANKL, receptor activator of nuclear factor- κ B ligand. Color images are available online.

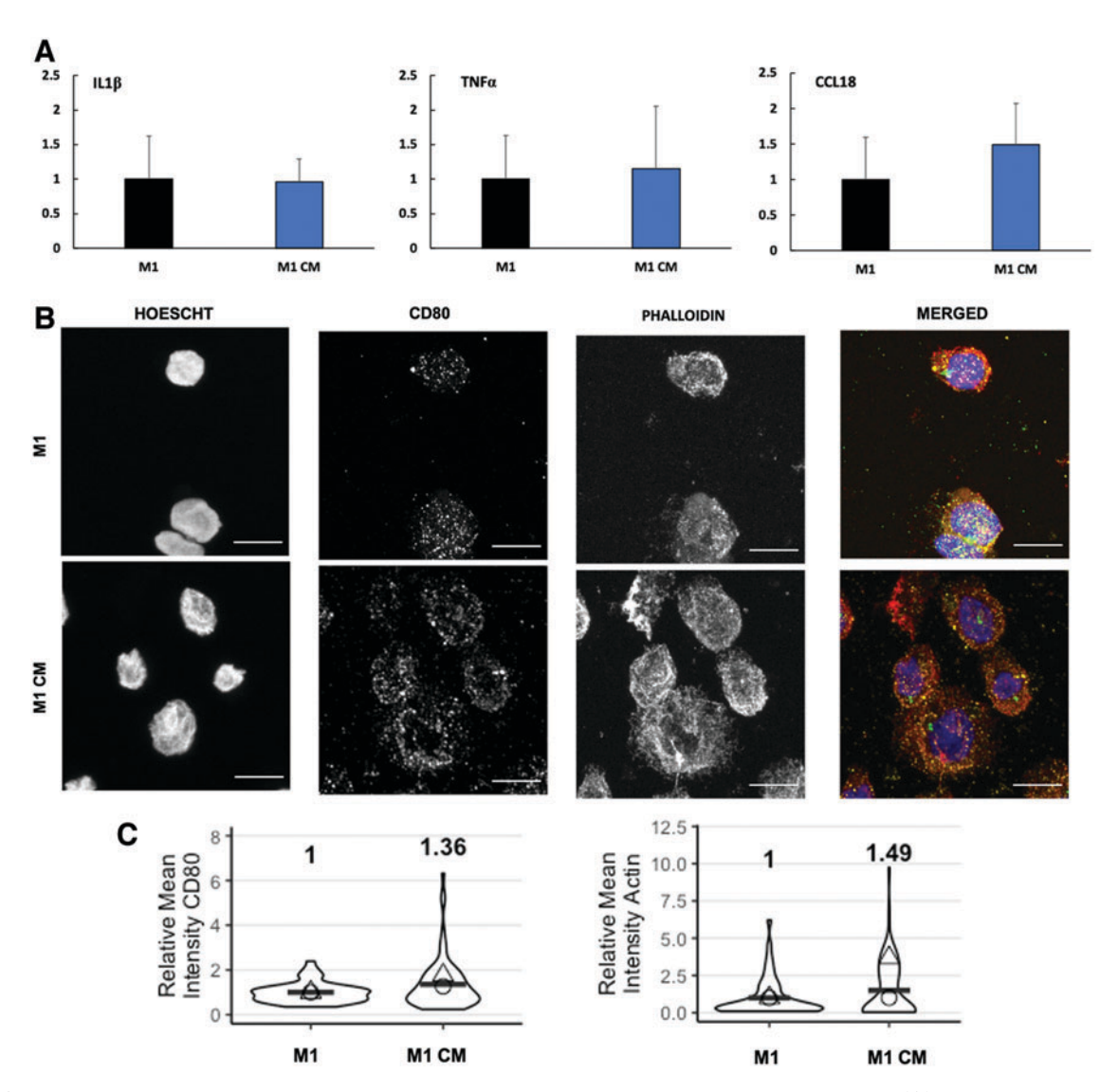


FIG. 4. Effect of osteoblast-derived conditioned media on macrophages phenotypic changes. **(A)** Gene expression of proand anti-inflammatory markers. **(B)** CD80 (*red*) and F-actin immunostaining (*green*), and nucleus staining (*blue*). The scale bar represents 10 μm. **(C)** The violin graphs demonstrate the relative mean intensity of at least three fields of view of CD80 and F-actin. F-actin, filamentous actin. Color images are available online.

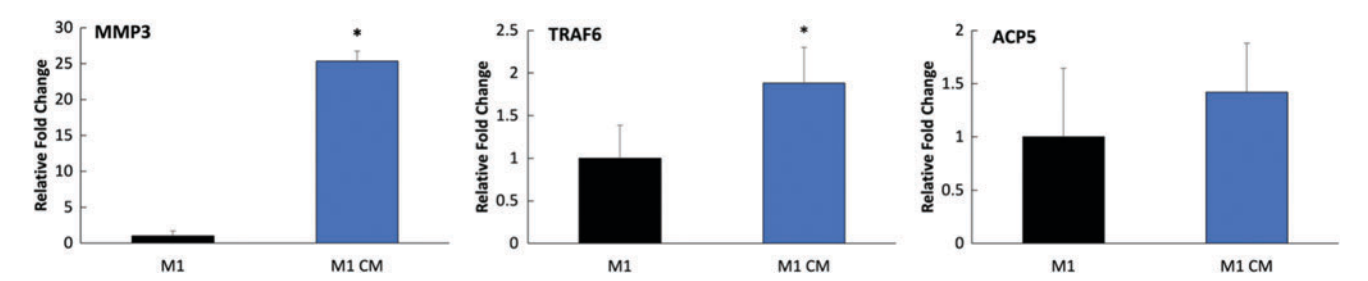


FIG. 5. Gene expressions of osteoclastogenic markers from macrophages cultured in conditioned media (CM) and complete macrophage media. The symbol "*" indicates significant difference with respect to M1 cells with p < 0.05 (n = 3). Color images are available online.

statistical differences in acid phosphatase 5, tartrate resistant (ACP5) expression between M1 and M1 CM macrophages. This is significant in terms of potential preosteoclast differentiation of macrophages due to osteoblast-derived conditioned media exposure because it is known that TRAF6 is particularly essential for osteoclast differentiation and maturation. ^{39–41}

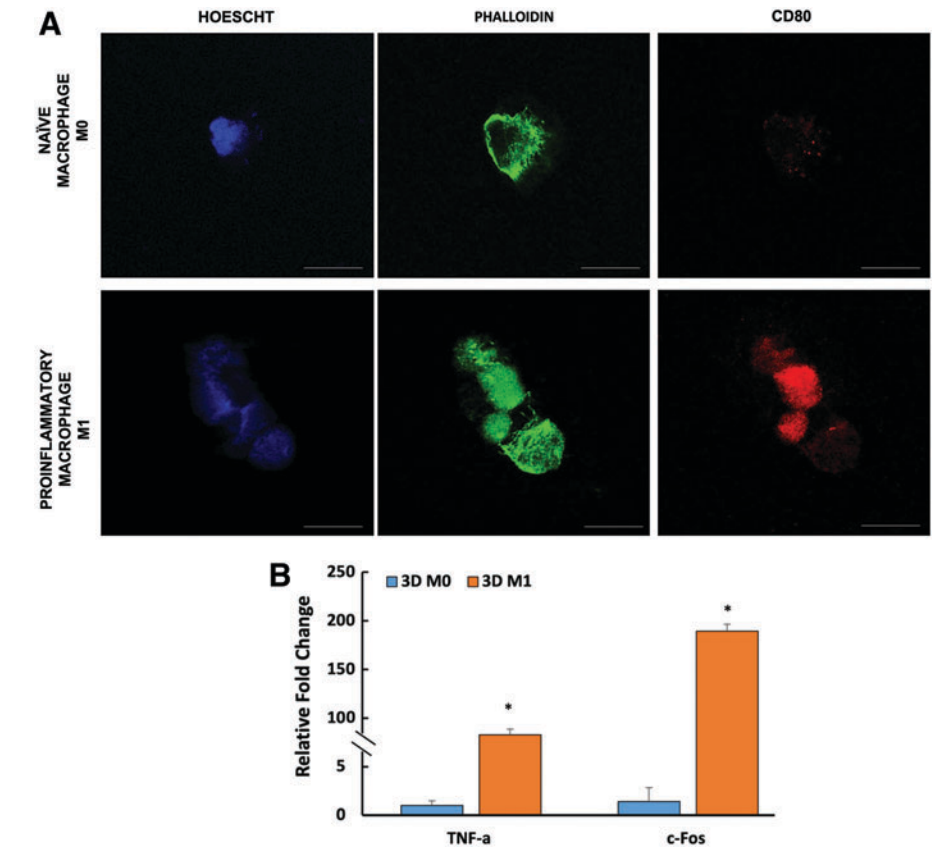
Macrophage-specific feedback on mature osteoblast

To understand the M1 macrophage-specific effect on mature osteoblasts, the osteoblasts were cultured with conditioned media from the M1 macrophage-laden 3D matrix (3D M1) for 7 days (Fig. 1). Before starting to collect conditioned media from 3D M1 culturing, the LPS-induced M1 polarization from naïve macrophages (M0) was confirmed using immunohistochemistry (Fig. 6A). The cell

nuclei, F-actin, and proinflammatory surface markers were tagged using DAPI, phalloidin, and CD80 antibody, respectively. Figure 6 demonstrated that proinflammatory CD80 expressed predominantly for M1 macrophages, which proved that proinflammatory macrophages were successfully differentiated from naïve macrophages (M0) using LPS.

Upon confirming the LPS-induced M1 differentiation, M1 macrophages were incorporated within the 3D collagen matrix to mimic the state of M1 after extravasating into the 3D matrix. Since TNF- α and c-FOS are the key transcription factors in RANKL-induced osteoclastogenesis, ^{42–44} the TNF- α and c-Fos expressions from the M1 within the 3D matrix (3D M1) were assessed and compared with naïve macrophages within a 3D collagen matrix. Figure 6B demonstrates that both TNF- α and c-Fos expressions were statistically significant (p<0.0001) upregulated for M1 macrophages within the 3D matrix compared to naïve macrophages (M0).

FIG. 6. (A) IHC staining for M1 marker CD80, cell nucleus with Hoechst (DAPI), and F-actin with phalloidin of naïve and proinflammatory macrophages. (B) Gene expressions of osteoclastogenic markers, TNF-α and c-FOS. Representative of 3 images/group (scale bar = $10 \mu m$). The symbol "*" indicates significant difference with p < 0.001(n=5). c-FOS, AP-1 transcription factor subunit; DAPI, 4',6-diamidino-2-phenylindole; TNF- α , tumor necrosis factor-alpha. Color images are available online.



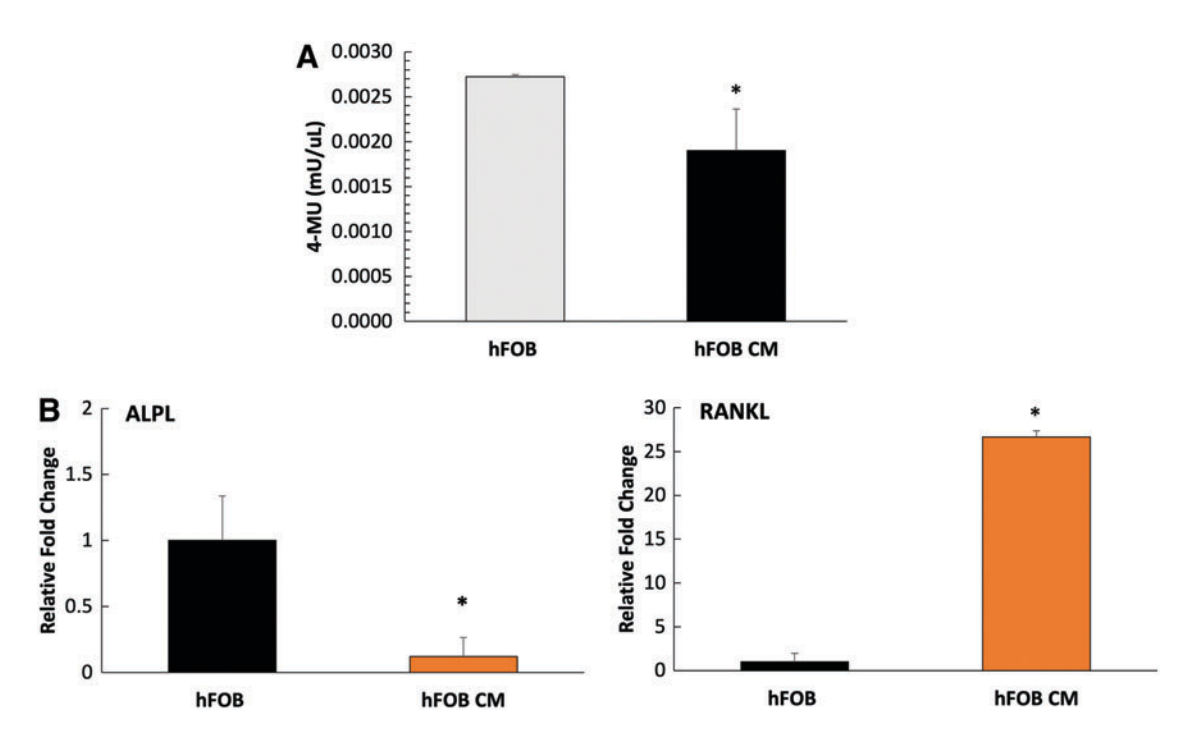


FIG. 7. Effect of macrophage-conditioned media on osteoblast cells. (A) ALP activity of osteoblast cells after conditioned media treatment. (B) Gene expression of ALPL and RANKL in osteoblast cells after conditioned media. The symbol "*" indicates significant difference with respect to osteoblast cells with p < 0.05 (n = 3). ALPL, alkaline phosphatase, biomineralization associated. Color images are available online.

Next, the effect of 3D M1-derived conditioned media on mature osteoblast was assessed regarding how secretome from M1 macrophages after extravasating into the 3D matrix affect the osteogenic activity of mature osteoblast. Specifically, the ALP activity and secretion of a vital osteoclastogenesis marker, transmembrane RANKL, by osteoblast cells were assessed. Figure 7 shows the ALP activity changes and gene expression of RANKL and alkaline phosphatase, biomineralization associated (ALPL) of mature osteoblasts when cultured with only osteogenic or macrophagic-conditioned media (CM).

The ALPL expression and ALP activity of osteoblasts exposed to 3D M1-conditioned media attenuated significantly compared to the osteoblast cultured with osteogenic media (Fig. 7B). On the other hand, the RANKL expression of osteoblast cultured with 3D M1-conditioned media increased significantly by almost 30-fold compared to counterparts from osteoblast cultured in regular osteogenic media (Fig. 7B). This significant increase (p<0.05) in RANKL expression would promote osteoclast differentiation of macrophages in close contact with mature osteoblast secretome since RANKL secreted by osteoblasts is essential for osteoclast formation and differentiation.

The effect of macrophages and osteoblast contact coculturing on individual cell type

To understand the effect of direct contact culturing of mature osteoblast and M1 macrophages on each cell type, the cells were encapsulated with the 3D collagen matrix and cultured for 7 days (Fig. 1). Before starting comprehensive biological characterization, the proximity of M1 and osteoblast within the 3D collagen matrix was confirmed using

histological analysis. Figure 8 shows the H&E (Fig. 8A) and Masson's trichrome (Fig. 8B) stained slides with M1 and osteoblasts. The histology images demonstrated two cell types with two distant morphologies. While the M1 macrophages exhibited a dot-like morphology (red circles in Fig. 8), osteoblasts showed a spread morphology (yellow arrows in Fig. 8). The osteoblasts and M1 macrophages were in close contact with the 3D collagen matrix.

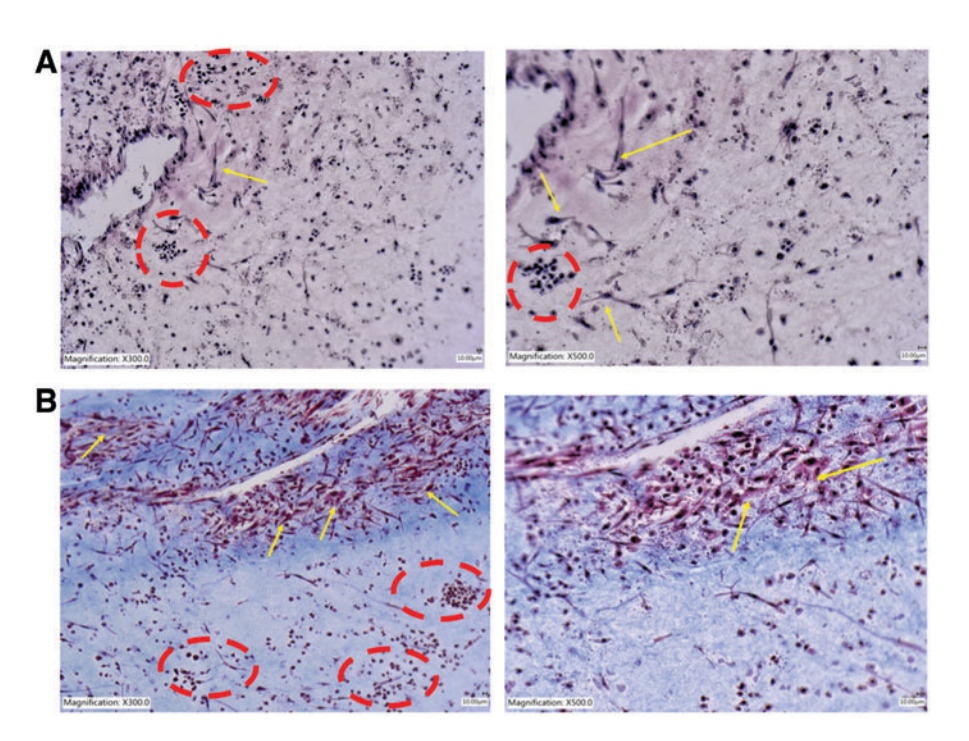
Upon confirming close contact of M1 and osteoblast cells, the effect of coculturing on M1 macrophages and osteoblast was investigated. Contact coculturing upregulated the macrophage's IL-1 β (a pro-inflammatory cytokine) mRNA expression while decreasing the CCL18 (anti-inflammatory marker) statistically significantly compared to macrophages cultured in a 3D matrix alone (Fig. 9A). There was no statistical upregulation in TNF- α between the cocultured macrophages and solo macrophage culturing groups. This suggested that M1 macrophages preserved their proinflammatory phenotype.

The IHC data (Fig. 9B) collected from proinflammatory surface protein CD80 further confirmed the gene expression results. The CD80 staining suggested that M1 macrophages still synthesized proinflammatory surface protein even though cocultured with osteoblast cells. Regarding the effect of co-culturing on osteoclast markers expression, the M1 macrophages within the coculture did not significantly express prominent osteoclastogenic markers (TRAF6 and ACP5), while MMP3 expression was downregulated. The data in Figure 9 implied that close contact with osteoblasts within the 3D matrix helped M1 macrophages preserve their phenotype without differentiating into osteoclast.

Coculturing with macrophages and osteoblast positively affected the encapsulated osteoblast's ALP activity. Figure 10A demonstrated that osteoblasts cultured with

FIG. 8. Histology images of osteoblasts and macrophages within a 3D matrix. (A) Representative hematoxylin and eosin staining of osteoblast and M1 macrophage cells within 3D matrix (300×and 500×magnification).

(B) Representative Masson's trichrome staining of osteoblast and M1 macrophage cells within 3D matrix (300×and 500×magnification). Dashed *red circles* point out macrophages, while *yellow arrows* point out the osteoblast cells. Color images are available online.



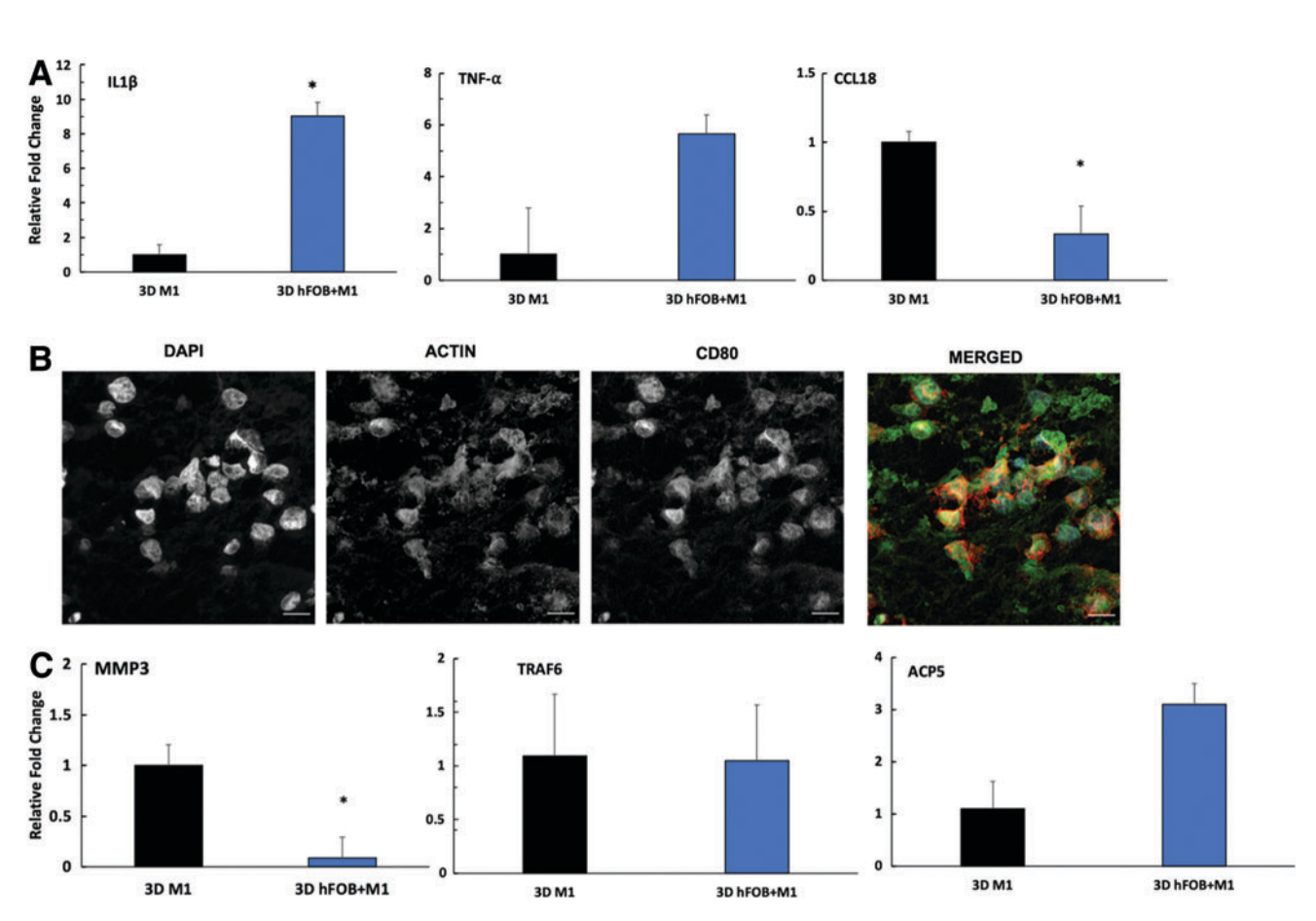


FIG. 9. Effect of direct coculturing of macrophage and osteoblast within 3D matrix on macrophages. (**A**) Gene expression of pro- and anti-inflammatory markers. The symbol "*" indicates significant difference with p < 0.05 (n = 3). (**B**) CD80 (red) and F-actin immunostaining (green), and nucleus staining (blue). Scale bar represents $10 \, \mu m$. (**C**) Gene expressions of osteoclastic markers. The symbol "*" indicates significant difference with p < 0.05 (n = 3). Color images are available online.

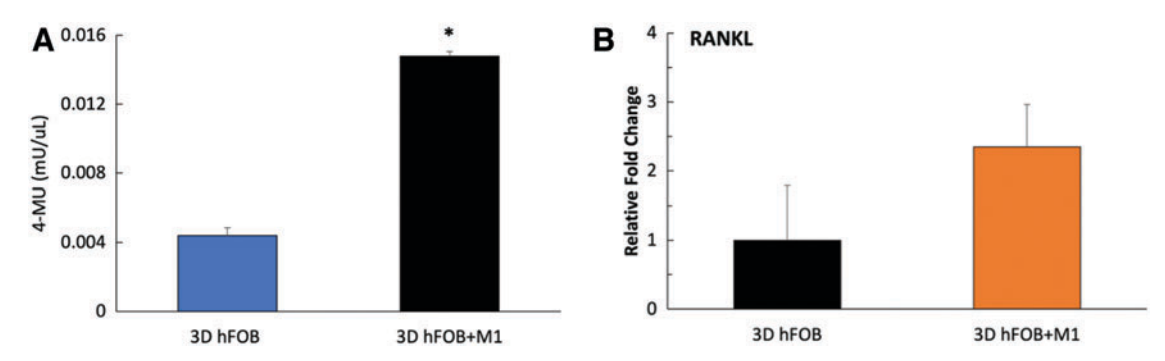


FIG. 10. Effect of direct coculturing of macrophages and osteoblast cells within a 3D matrix. (A) ALP activity of osteoblast-encapsulated 3D matrix and direct culture of macrophages and osteoblast cells 3D matrix. (B) Gene expression of osteoclast activity (RANKL) in the osteoblast-encapsulated 3D matrix and direct culture of macrophages and osteoblast cells 3D matrix. The symbol "*" indicates significant difference with respect to osteoblast cells with p < 0.05 (n = 3). Color images are available online.

macrophages with the 3D matrix had an enhanced ALP activity compared to counterparts cultured in the 3D matrix alone. There was no statistical upregulation in RANKL expression between the cocultured osteoblasts and osteoblasts cultured alone in the 3D matrix (Fig. 10B). The coculturing data suggested that contact culturing of M1 macrophages and osteoblast created an anabolic effect on osteogenesis.

Discussion

Evidence suggests that macrophages and osteoblasts interact and influence each other's function during osteolytic diseases. The osteoblasts have been shown to secrete various factors, such as RANKL and macrophage colony-stimulating factor, which can stimulate the differentiation of macrophages into osteoclasts. Similarly, proinflammatory macrophages modulate osteogenic activities, including ALP synthesis and mineralization. Thus, the complex and multifaceted crosstalk between M1 macrophages and osteoblast modulates the balance between osteogenesis and osteoclastogenesis.

In osteoblast-macrophage interaction studies, a tremendous effort has been put into understanding the effects of macrophages on osteoblasts in response to abrasive prosthetic wear particles exposure and bacterial infection, and mediators released by osteoblasts to act on macrophages using 2D *in vitro* platforms including transwell plate and petri dish culturing. The three-dimensionality of the extracellular environment circulating the macrophages and osteoblasts and its effect on the macrophage-osteoblast interaction should be addressed. Yet, it is well established that osteoblast and macrophage function (proliferation, differentiation, migration, etc.) entirely differently in a 3D microenvironment than in 2D surfaces. ^{50–53}

In this study, the proinflammatory macrophage and osteoblast interaction was investigated with contact coculturing and contact-independent (conditioned media) culturing using 3D collagen matrix with extravasated macrophages and 3D mineralized matrix with residing osteoblasts and 3D matrix with proinflammatory macrophages and osteoblasts. The comprehensive biomimetic approach has helped us to decipher cell-specific effects on osteogenesis and osteoclastogenesis during osteolytic pathological conditions, including periodontitis. ⁵²

To understand the osteoblast (hFOB)-specific effect on proinflammatory macrophages, the conditioned media from an osteoblast-laden 3D mineralized matrix was utilized for culturing proinflammatory macrophages (Fig. 1). First, the mineralized matrix formation within the 3D hFOB-laden matrix was confirmed using structural, spectral, and biological analyses (Fig. 2) before starting the conditioned media experiment. The calcium deposition and mineralization within the 3D matrix by encapsulated osteoblasts were observed by increased calcium peaks in spectral analysis (Fig. 2B), calcium mapping within the 3D matrix (Fig. 2C), and von Kossa-stained histological slides (Fig. 2E, F). The osteoblast ALP activity (Fig. 2D) within the 3D matrix also increased compared to the control (osteoblast cultured on a 2D surface). The results in Figure 2 overall convinced that the 3D in vitro platform could mimic the osteoblast-laden mineralized matrix.

The 3D osteoblast-laden matrix (3D hFOB) was used in further analysis to identify the solo effect of osteoblast's indirect interaction on macrophages and to understand whether osteoblast-derived secretome from the mineralized matrix would change the phenotypic commitment of proinflammatory macrophages. While the osteoblast-derived conditioned media was collected for macrophage culturing, the expression of prominent osteoclastogenic markers from encapsulated osteoblasts was analyzed. The NF-κB modulates the differentiation or activity of osteoclasts and proinflammatory macrophages, 4,54 and the RANKL expression from osteoblast is necessary for macrophage differentiation toward preosteoclast. 4,40,44,51,55 Figure 3 demonstrated that while NF-κB expressions increased for osteoblast cells within the mineralized matrix, the RANKL expressions did not significantly change. This result was reflected in the phenotypic changes in macrophages cultured with osteoblast-derived conditioned media (M1 CM).

Although the phenotypic commitment of macrophages is transient depending on the circulating environment, $^{56-58}$ the macrophages cultured with osteoblast-derived conditioned media preserved their proinflammatory phenotype. Figure 4A demonstrated that the expression of proinflammatory (TNF- α and IL-1 β) and anti-inflammatory markers (CCL18) did not significantly change for M1 CM groups compared to macrophages cultured with regular complete media (M1). This data

was further confirmed with the IHC images (Fig. 4B, C) of CD80 cell surface protein expressed by proinflammatory cells. The amount of CD80 protein was not different for macrophages cultured with osteoblast-conditioned media (M1 CM) than the counterparts cultured with the complete media (M1). The expressions of osteoclastogenic markers (TRAF and ACP5) also did not change between the M1 CM and M1 groups. This can be attributed to osteoblasts' NF-κB and RANKL expressions within the mineralized matrix (3D hFOB) (Fig. 3). The RANKL is essential for initiating osteoclastogenesis, yet the RANKL expression did not upregulate for 3D hFOB. Thus, it was expected to have no significant changes in the expression of osteoclastogenic markers (TRAF and ACP5) from macrophages cultured with the conditioned media collected from these cells. It can be concluded that the indirect interaction of osteoblasts within the mineralized matrix does not differentiate the proinflammatory macrophages from anti-inflammatory lineage or preosteoclast through paracrine factors. Instead, it helps proinflammatory macrophages to maintain the status quo regarding the proinflammatory phenotype.

To understand the proinflammatory macrophage-specific effect on osteoblast, the conditioned media from a proinflammatory macrophage-laden 3D collagen matrix was utilized for culturing osteoblast (Fig. 1). The bacteria-induced proinflammatory macrophages were encapsulated within the 3D collagen matrix to mimic the state of macrophages after extravasating within the tissue and differentiate into proinflammatory phenotypes. First, we confirmed the bacteriainduced differentiation of naïve macrophages (M0) toward proinflammatory macrophages (M1). Figure 6A demonstrated the enhanced proinflammatory cell surface protein CD80 synthesis for M1 macrophages compared to M0 macrophages, which proved that the macrophages encapsulated within the 3D collagen matrix had a proinflammatory phenotype. Then, the TNF-α and c-FOS expression from encapsulated proinflammatory macrophages were studied before starting the conditioned media experiment.

TNF-α and c-FOS are important osteoclastogenic-related markers, which promote macrophage polarization to osteoclast and stimulate osteoblast cells to express RANKL, which push preosteoclast differentiation of macro-phages. 42,44,55,59 Figure 6B shows that the mRNA expression of osteoclastogenic markers, c-Fos, and TNF-α upregulated 180-fold and 80-fold for proinflammatory macrophages within the 3D collagen (3D M1) matrix compared to naïve macrophages within the collagen matrix (3D M0). This means that the conditioned media from 3D M1 used for osteoblast culturing could start a vicious cycle promoting RANKL expression from osteoblasts, further promoting the differentiation of macrophages toward osteoclasts. Figure 7 further confirmed the fact that the ALPL expression at the molecular level and the ALP activity of osteoblasts cultured with macrophage-derived conditioned media (hFOB CM) dropped significantly (p < 0.05) compared to counterparts cultured with complete media (hFOB). At the same time, the RANKL expression increased more than 25-fold for hFOB CM groups.

Overall, secretome from the proinflammatory macrophageladen 3D collagen matrix culturing promotes osteoclastogenesis. The proinflammatory macrophage-derived conditioned media demonstrated how proinflammatory macrophages, upon extravasating into 3D tissue, may create indirect interaction with osteoblast through paracrine factor and promote osteo-clastogenesis through themselves not only expressing osteo-clastogenic markers but also stimulating osteoblast cells to express RANKL which promotes further osteoclastogenic differentiation of macrophages through RANKL/RANK axis.⁴³

From osteoblast-derived and inflammatory macrophage-derived conditioned media studies, it was demonstrated that while macrophages are dominant players in osteoclastogenesis by increasing osteoclastogenic markers for osteoblasts and macrophages and reducing the osteoblastic activities (ALP activity), the osteoblasts did not promote osteoclast differentiation. The next obvious question was whether osteoblast would curb the osteoclastogenic effect of macrophages when they are both in cell-to-cell contact culturing. To address this question, the proinflammatory macrophages and osteoblasts are encapsulated within a 3D collagen matrix in a 1:1 ratio and cultured together (Fig. 1).

After we confirmed that proinflammatory macrophages and osteoblast cells were grown in close physical proximity within the 3D collagen matrix (Fig. 8), the effect of contact culturing on proinflammatory macrophages and osteoblasts was investigated. The results were quite exciting. For M1 macrophages within the 3D coculture, the TNF- α and IL-1 β (proinflammatory markers) expressions were upregulated, while CCL18 mRNA expressions were downregulated when osteoclastogenic markers (TRAF6 and ACP5) were not changed (Fig. 9). The data suggested that the osteoblasts curbed the osteoclastogenic differentiation of macrophages while macrophages still preserved their proinflammatory lineages. The osteoblast within the 3D coculture demonstrated increased ALP activity and did not express RANKL significantly different than the osteoblast cultured within a 3D collagen matrix without macrophages (Fig. 10) which was an improvement compared to osteoblast cultured with macrophage-derived conditioned media (Fig. 6). Based on these findings, it can be inferred that the interaction between osteoblasts and proinflammatory macrophages within the 3D matrix may positively impact bone tissue.

It is essential to conduct further comprehensive investigations involving a wider range of cells to fully elucidate the underlying mechanisms and confirm the extent of this effect. The complex interplay between osteoblasts and proinflammatory macrophages within the 3D matrix warrants further study to understand better their potential contributions to bone tissue homeostasis and regeneration.

In addition, although it was not the study's primary goal, we have also proved how osteoblasts behave differently on the 2D surface than when encapsulated within the 3D matrix when osteoclast cultured on a 2D surface served as a control (Figs. 2D and 3). This finding further proved the importance of the 3D biomimetic approach *in vitro* modeling in macrophage-osteoblast interaction studies.

In periodontitis, the destruction in bone remodeling toward bone resorption is due to the differentiation of bacteria-derived proinflammatory macrophages into osteoclasts. We have used periodontitis as a case study. Yet, the study's outcome can be applied to osteolytic diseases in which bacteria-derived macrophages and osteoblast crosstalk. Overall, the role of interaction between bacteria-induced proinflammatory macrophages and osteoblast in periodontitis is complex and multifaceted, and further

mechanistic studies are needed to fully understand the mechanisms by which these cells contribute to the development and progression of the disease.

Conclusion

While animal models are a great platform to study the complex and multifaceted interaction between the proinflammatory macrophage and osteoblast in their native environment, the animals demonstrate different metabolic responses leading to variation in results. In contrast, welldefined and controlled biomimetic 3D in vitro models can be used to understand the cell-specific and synergetic effect of pro-inflammatory macrophage and osteoblasts in osteolytic diseases. The current study sheds light on understanding the dominant players in direct and indirect macrophageosteoblast interaction using biomimetic 3D cell-laden matrices. While M1 macrophage-derived conditioned media had a catabolic effect on osteoclastogenesis, osteoblastderived conditioned media helped M1 macrophages preserve their inflammatory phenotype without enhancing osteoclastogenic marker expressions. In contact coculturing, osteoblast curbed the pro-osteoclastogenic potential of macrophage differentiation.

Acknowledgments

We thank the University of Toledo, Center for Materials and Senser Characterization, for their access to the scanning electron microscope and assistance. We thank Dr. Xiaohon Li for generously providing the hFOB and hFOB-GFP cell lines. We sincerely appreciate their contribution to our research.

Authors' Contributions

E.Y.-A., D.J., R.O., and M.T. conceived and planned the experiments. D.J. carried out the experiments. D.J. and E.Y.-A. analyzed and interpreted the data. A.R. and R.G.-M. contributed to confocal image acquisition. A.R. contributed to image data analysis. P.B. contributed to fluorescence image acquisition. E.Y.-A. and D.J. wrote the main article text. All authors reviewed and agreed to the final version of the article.

Disclosure Statement

All the authors declare that they have no conflicts of interest.

Funding Information

This study is supported by the National Science Foundation under Grant 2213958 (E.Y.-A.) and by the National Institute of Health and Grant R01GM136826 (R.G.-M.).

References

- Herrera D, Matesanz P, Martin C, et al. Adjunctive effect of locally delivered antimicrobials in periodontitis therapy: A systematic review and meta-analysis. J Clin Periodontol 2020;47 Suppl 22:239–256; doi: 10.1111/jcpe.13230
- Khosravimelal S, Chizari M, Farhadihosseinabadi B, et al. Fabrication and characterization of an antibacterial chitosan/silk fibroin electrospun nanofiber loaded with a cationic

- peptide for wound-dressing application. J Mater Sci Mater Med 2021;32(9):114; doi: 10.1007/s10856-021-06542-6
- 3. Varin A, Gordon S. Alternative activation of macrophages: Immune function and cellular biology. Immunobiology 2009;214(7):630–641; doi: 10.1016/j.imbio.2008.11.009
- Lampiasi N, Russo R, Zito F. The alternative faces of macrophage generate osteoclasts. Biomed Res Int 2016;2016:9089610; doi: 10.1155/2016/9089610
- Renvert S, Widen C, Persson RG. Cytokine and microbial profiles in relation to the clinical outcome following treatment of peri-implantitis. Clin Oral Implants Res 2017;28(9):1127–1132; doi: 10.1111/clr.12927
- Renvert S, Widen C, Persson GR. Cytokine expression in peri-implant crevicular fluid in relation to bacterial presence. J Clin Periodontol 2015;42(7):697–702; doi: 10.1111/ jcpe.12422
- Bezgin T, Yilmaz AD, Celik BN, et al. Efficacy of plateletrich plasma as a scaffold in regenerative endodontic treatment. J Endod 2015;41(1):36–44; doi: 10.1016/j.joen.2014.10.004
- Kim JS, Choi M, Choi JY, et al. Implication of the association of fibrinogen citrullination and osteoclastogenesis in bone destruction in rheumatoid arthritis. Cells 2020;9(12); doi: 10.3390/cells9122720
- 9. Bost KL, Bento JL, Ellington JK, et al. Induction of colonystimulating factor expression following Staphylococcus or Salmonella interaction with mouse or human osteoblasts. Infect Immun 2000;68(9):5075–5083; doi: 10.1128/IAI.68 .9.5075-5083.2000
- Liu X, Bao C, Xu HHK, et al. Osteoprotegerin genemodified BMSCs with hydroxyapatite scaffold for treating critical-sized mandibular defects in ovariectomized osteoporotic rats. Acta Biomater 2016;42:378–388; doi: 10 .1016/j.actbio.2016.06.019
- 11. Kobayashi N, Kadono Y, Naito A, et al. Segregation of TRAF6-mediated signaling pathways clarifies its role in osteoclastogenesis. EMBO J 2001;20(6):1271–1280; doi: 10.1093/emboj/20.6.1271
- Song G, Wang S, Barkestani MN, et al. Membrane attack complexes, endothelial cell activation, and direct allorecognition. Front Immunol 2022;13:1020889; doi: 10 .3389/fimmu.2022.1020889
- Fan S, Sun X, Su C, et al. Macrophages-bone marrow mesenchymal stem cells crosstalk in bone healing. Front Cell Dev Biol 2023;11:1193765; doi: 10.3389/fcell.2023.1193765
- 14. Lu D, Xu Y, Liu Q, et al. Mesenchymal stem cell-macrophage crosstalk and maintenance of inflammatory microenvironment homeostasis. Front Cell Dev Biol 2021;9:681171; doi: 10.3389/fcell.2021.681171
- 15. Valles G, Bensiamar F, Maestro-Paramio L, et al. Influence of inflammatory conditions provided by macrophages on osteogenic ability of mesenchymal stem cells. Stem Cell Res Ther 2020;11(1):57; doi: 10.1186/s13287-020-1578-1
- 16. Valles G, Gil-Garay E, Munuera L, et al. Modulation of the cross-talk between macrophages and osteoblasts by titanium-based particles. Biomaterials 2008;29(15):2326–2335; doi: 10.1016/j.biomaterials.2008.02.011
- 17. Ponzetti M, Rucci N. Updates on osteoimmunology: What's new on the cross-talk between bone and immune system. Front Endocrinol (Lausanne) 2019;10:236; doi: 10.3389/fendo.2019.00236
- 18. Kumar G, Roger PM. From crosstalk between immune and bone cells to bone erosion in infection. Int J Mol Sci 2019;20(20); doi: 10.3390/ijms20205154

 Vis MAM, Zhao F, Bodelier ESR, et al. Osteogenesis and osteoclastogenesis on a chip: Engineering a self-assembling 3D coculture. Bone 2023;173:116812; doi: 10.1016/j.bone .2023.116812

- Tang H, Husch JFA, Zhang Y, et al. Coculture with monocytes/macrophages modulates osteogenic differentiation of adipose-derived mesenchymal stromal cells on poly(lactic-co-glycolic) acid/polycaprolactone scaffolds. J Tissue Eng Regen Med 2019;13(5):785–798; doi: 10 .1002/term.2826
- Shanbhag S, Rana N, Suliman S, et al. Influence of bone substitutes on mesenchymal stromal cells in an inflammatory microenvironment. Int J Mol Sci 2022;24(1); doi: 10 .3390/ijms24010438
- 22. Romero-Lopez M, Li Z, Rhee C, et al. Macrophage effects on mesenchymal stem cell osteogenesis in a three-dimensional in vitro bone model. Tissue Eng Part A 2020;26(19–20):1099–1111; doi: 10.1089/ten.TEA.2020.0041
- Pathak JL, Bravenboer N, Verschueren P, et al. Inflammatory factors in the circulation of patients with active rheumatoid arthritis stimulate osteoclastogenesis via endogenous cytokine production by osteoblasts. Osteoporos Int 2014;25(10):2453–2463; doi: 10.1007/s00198-014-2779-1
- Luo ML, Jiao Y, Gong WP, et al. Macrophages enhance mesenchymal stem cell osteogenesis via down-regulation of reactive oxygen species. J Dent 2020;94:103297; doi: 10 .1016/j.jdent.2020.103297
- Loi F, Cordova LA, Zhang R, et al. The effects of immunomodulation by macrophage subsets on osteogenesis in vitro. Stem Cell Res Ther 2016;7:15; doi: 10.1186/s13287-016-0276-5
- Li Y, Kong N, Li Z, et al. Bone marrow macrophage M2 polarization and adipose-derived stem cells osteogenic differentiation synergistically promote rehabilitation of bone damage. J Cell Biochem 2019;120(12):19891–19901; doi: 10.1002/jcb.29297
- 27. He XT, Wu RX, Xu XY, et al. Macrophage involvement affects matrix stiffness-related influences on cell osteogenesis under three-dimensional culture conditions. Acta Biomater 2018;71:132–147; doi: 10.1016/j.actbio.2018.02.015
- 28. Gong L, Zhao Y, Zhang Y, et al. The macrophage polarization regulates MSC osteoblast differentiation in vitro. Ann Clin Lab Sci 2016;46(1):65–71.
- 29. Elango J, Sanchez C, de Val J, et al. Cross-talk between primary osteocytes and bone marrow macrophages for osteoclastogenesis upon collagen treatment. Sci Rep 2018;8(1):5318; doi: 10.1038/s41598-018-23532-x
- 30. Ehnert S, van Griensven M, Unger M, et al. Co-culture with human osteoblasts and exposure to extremely low frequency pulsed electromagnetic fields improve osteogenic differentiation of human adipose-derived mesenchymal stem cells. Int J Mol Sci 2018;19(4); doi: 10.3390/ijms19040994
- Deng M, Tan J, Dai Q, et al. Macrophage-mediated bone formation in scaffolds modified with MSC-derived extracellular matrix is dependent on the migration inhibitory factor signaling pathway. Front Cell Dev Biol 2021;9: 714011; doi: 10.3389/fcell.2021.714011
- 32. Bernhardt A, Thieme S, Domaschke H, et al. Crosstalk of osteoblast and osteoclast precursors on mineralized collagen—towards an in vitro model for bone remodeling.

- J Biomed Mater Res A 2010;95(3):848–856; doi: 10.1002/jbm.a.32856
- 33. Angelova Volponi A, Kawasaki M, Sharpe PT. Adult human gingival epithelial cells as a source for whole-tooth bioengineering. J Dent Res 2013;92(4):329–334; doi: 10.1177/0022034513481041
- Orecchioni M, Ghosheh Y, Pramod AB, et al. Macrophage polarization: Different gene signatures in M1(LPS+) vs. classically and M2(LPS-) vs. alternatively activated macrophages. Front Immunol 2019;10:1084; doi: 10.3389/fimmu.2019.01084
- 35. Tintut Y, Patel J, Territo M, et al. Monocyte/macrophage regulation of vascular calcification in vitro. Circulation 2002;105(5):650–655; doi: 10.1161/hc0502.102969
- 36. Novack DV. Role of NF-kappaB in the skeleton. Cell Res 2011;21(1):169–182; doi: 10.1038/cr.2010.159
- 37. Walsh MC, Choi Y. Biology of the RANKL-RANK-OPG system in immunity, bone, and beyond. Front Immunol 2014;5:511; doi: 10.3389/fimmu.2014.00511
- 38. Raggi F, Pelassa S, Pierobon D, et al. Regulation of human macrophage M1–M2 polarization balance by hypoxia and the triggering receptor expressed on myeloid cells-1. Front Immunol 2017;8:1097; doi: 10.3389/fimmu.2017.01097
- 39. Wan J, Zhang G, Li X, et al. Matrix metalloproteinase 3: A promoting and destabilizing factor in the pathogenesis of disease and cell differentiation. Front Physiol 2021;12: 663978; doi: 10.3389/fphys.2021.663978
- Kim EN, Kwon J, Lee HS, et al. Inhibitory effect of cudratrixanthone U on RANKL-induced osteoclast differentiation and function in macrophages and BMM cells. Front Pharmacol 2020;11:1048; doi: 10.3389/fphar.2020.01048
- Guo J, Cao X, Ma X, et al. Tumor necrosis factor receptorassociated factor 6 (TRAF6) inhibition modulates bone loss and matrix metalloproteinase expression levels in collageninduced rheumatoid arthritis rat. Ann Palliat Med 2020;9(6):4017–4028; doi: 10.21037/apm-20-1894
- 42. Huang H, Chang EJ, Ryu J, et al. Induction of c-Fos and NFATc1 during RANKL-stimulated osteoclast differentiation is mediated by the p38 signaling pathway. Biochem Biophys Res Commun 2006;351(1):99–105; doi: 10.1016/j.bbrc.2006.10.011
- 43. Yao Z, Lei W, Duan R, et al. RANKL cytokine enhances TNF-induced osteoclastogenesis independently of TNF receptor associated factor (TRAF) 6 by degrading TRAF3 in osteoclast precursors. J Biol Chem 2017;292(24):10169–10179; doi: 10.1074/jbc.M116.771816
- 44. Luo G, Li F, Li X, et al. TNF-alpha and RANKL promote osteoclastogenesis by upregulating RANK via the NF-kappaB pathway. Mol Med Rep 2018;17(5):6605–6611; doi: 10.3892/mmr.2018.8698
- 45. Manolagas SC, Jilka RL. Bone marrow, cytokines, and bone remodeling. Emerging insights into the pathophysiology of osteoporosis. N Engl J Med 1995;332(5):305–311; doi: 10.1056/NEJM199502023320506
- Hofbauer LC, Heufelder AE. Role of receptor activator of nuclear factor-kappaB ligand and osteoprotegerin in bone cell biology. J Mol Med (Berl) 2001;79(5–6):243–253; doi: 10.1007/s001090100226
- 47. Freundlich M, Alonzo E, Bellorin-Font E, et al. Increased osteoblastic activity and expression of receptor activator of NF-kappaB ligand in nonuremic nephrotic syndrome. J Am Soc Nephrol 2005;16(7):2198–2204; doi: 10.1681/ASN .2004121062

- 48. Liu G, Xu G, Gao Z, et al. Demineralized dentin matrix induces odontoblastic differentiation of dental pulp stem cells. Cells Tissues Organs 2016;201(1):65–76; doi: 10.1159/000440952
- 49. Chen X, Dou J, Fu Z, et al. Macrophage M1 polarization mediated via the IL-6/STAT3 pathway contributes to apical periodontitis induced by *Porphyromonas gingivalis*. J Appl Oral Sci 2022;30:e20220316; doi: 10.1590/1678-7757-2022-0316
- Adams S, Wuescher LM, Worth R, et al. Mechanoimmunomodulation: Mechanoresponsive changes in macrophage activity and polarization. Ann Biomed Eng 2019;47(11):2213–2231; doi: 10.1007/s10439-019-02302-4
- 51. Osorio R, Alfonso-Rodriguez CA, Osorio E, et al. Novel potential scaffold for periodontal tissue engineering. Clin Oral Investig 2017;21(9):2695–2707; doi: 10.1007/s00784-017-2072-8
- 52. Osorio R, Alfonso-Rodriguez CA, Medina-Castillo AL, et al. Bioactive polymeric nanoparticles for periodontal therapy. PLoS One 2016;11(11):e0166217; doi: 10.1371/journal.pone.0166217
- 53. Jacho D, Rabino A, Garcia-Mata R, et al. Mechanoresponsive regulation of fibroblast-to-myofibroblast transition in three-dimensional tissue analogues: Mechanical strain amplitude dependency of fibrosis. Sci Rep 2022;12(1):16832; doi: 10.1038/s41598-022-20383-5
- 54. Yilmaz M, Demir E, Firatli Y, et al. Tissue levels of CD80, CD163 and CD206 and their ratios in periodontal and perimplant health and disease. Curr Issues Mol Biol 2022;44(10):4704–4713; doi: 10.3390/cimb44100321
- 55. Kobayashi K, Takahashi N, Jimi E, et al. Tumor necrosis factor alpha stimulates osteoclast differentiation by a

- mechanism independent of the ODF/RANKL-RANK interaction. J Exp Med 2000;191(2):275–286; doi: 10.1084/jem.191.2.275
- 56. Wynn TA. Cellular and molecular mechanisms of fibrosis. J Pathol 2008;214(2):199–210; doi: 10.1002/path.2277
- Pakshir P, Alizadehgiashi M, Wong B, et al. Dynamic fibroblast contractions attract remote macrophages in fibrillar collagen matrix. Nat Commun 2019;10(1):1850; doi: 10.1038/s41467-019-09709-6
- Shortridge C, Akbari Fakhrabadi E, Wuescher LM, et al. Impact of digestive inflammatory environment and genipin crosslinking on immunomodulatory capacity of injectable musculoskeletal tissue scaffold. Int J Mol Sci 2021;22(3); doi: 10.3390/ijms22031134
- 59. Kitaura H, Kimura K, Ishida M, et al. Immunological reaction in TNF-alpha-mediated osteoclast formation and bone resorption in vitro and in vivo. Clin Dev Immunol 2013;2013:181849; doi: 10.1155/2013/181849

Address correspondence to: Eda Yildirim-Ayan, PhD Department of Bioengineering University of Toledo 2801 West Bancroft Toledo, OH 43606 USA

E-mail: eda.yildirimayan@utoledo.edu

Received: May 10, 2023 Accepted: August 9, 2023

Online Publication Date: October 5, 2023